Direct observation of reaction intermediates for a well defined heterogeneous alkene metathesis catalyst

Frédéric Blanc[†], Romain Berthoud[†], Christophe Copéret[†‡], Anne Lesage[§], Lyndon Emsley[§], Rojendra Singh[¶], Thorsten Kreickmann[¶], and Richard R. Schrock[¶]

[†]Université de Lyon, Institut de Chimie de Lyon, Laboratoire de Chimie, Catalyse, Polymères, et Procédés, Equipe Chimie Organométallique de Surface, Ecole Supérieure Chimie Physique Électronique de Lyon/Centre National de la Recherche Scientifique/Université Lyon 1, 43 boulevard du 11 Novembre, 69616 Villeurbanne Cedex, France; [§]Centre de RMN à Très Hauts Champs, Université de Lyon/Centre National de la Recherche Scientifique/Ecole Normale Supérieure de Lyon/Université Claude Bernard Lyon 1, 5 rue de la Doua, 69100 Villeurbanne, France; and [¶]Department of Chemistry, Massachusetts Institute of Technology, Cambridge, MA 02139

Edited by John Bercaw, California Institute of Technology, Pasadena, CA, and approved May 19, 2008 (received for review March 5, 2008)

Grafting of $[W(\equiv NAr)(=CHtBu)(2,5\text{-}Me_2NC_4H_2)_2]$ on a silica partially dehydroxylated at 700°C ($SiO_{2\text{-}(700)}$) generates the corresponding monosiloxy complex $[(\equiv SiO)W(\equiv NAr)(=CHtBu)(2,5\text{-}Me_2NC_4H_2)]$ as the major species (≈90%) along with $[(\equiv SiO)W(\equiv NAr)(CH_2tBu)(2,5\text{-}Me_2NC_4H_2)_2]$, according to mass balance analysis, IR, and NMR studies. This heterogeneous catalyst displays good activity and stability in the metathesis of propene. Very importantly, solid state NMR spectroscopy allows observation of the propagating alkylidene as well as stable metallacyclobutane intermediates. These species have the same reactivity as the initial surface complex $[(\equiv SiO)W(\equiv NAr)(=CHtBu)(2,5\text{-}Me_2NC_4H_2)]$, which shows that they are the key intermediates of alkene metathesis.

alkylidene | heterogeneous catalysis | metallacyclobutanes | solid state NMR

Alkene metathesis, a key reaction in industry, is used for the synthesis of both basic and fine chemicals as well as polymers (1–3). Because of an increasing world demand for propene, one of the most important processes involving metathesis is now the synthesis of propene through cross-metathesis of ethene and 2-butene. This process relies on heterogeneous catalysis because of its many technical and economical advantages. However, the development of more efficient systems in terms of activity, selectivity, and stability is still required because of the need to optimize the use of resources within the context of a more sustainable development. Although several breakthroughs in the preparation and characterization of single-site heterogeneous catalysts have already appeared (4–7), including those in the field of alkene metathesis catalysts (8–15), understanding deactivation phenomena is still a challenge today. In this respect, the observation and determination of the fate of reaction intermediates would help tackle this problem and thereby lead to improved catalyst performances. In the specific case of alkene metathesis, it has been proposed that carbenes and metallacyclobutanes are key reaction intermediates (16). Although they have been unambiguously prepared and observed for homogeneous catalysts (17–29), observing them as heterogeneous catalysts has proved to be a formidable challenge (30–32). Note that because the surface can play such a crucial role, one should never assume that the intermediates are identical in heterogeneous and homogeneous systems (31, 32). Currently, whereas well defined highly active silica supported metallocarbene precursors having neopentylidene and neophylidene ligands can be prepared and characterized at a molecular level, observation of propagating alkylidene or metallacyclobutanes have remained elusive even for these well defined systems (33).

Here, we describe the preparation of a well defined silica supported W alkylidene species $[(\equiv SiO)W(\equiv NAr)(=CHtBu)(2,5\text{-}Me_2NC_4H_2)]$ (compound **1**), report its activity in alkene metathesis, observe the methylidene and metallacyclobutane species, and show they are key reaction intermediates in alkene metathesis.

Results and Discussion

Grafting $[W(\equiv NAr)(=CHtBu)(2,5\text{-}Me_2NC_4H_2)_2]$ (compound **2**) (34) on a silica that has been partially dehydroxylated at 700°C ($SiO_{2\text{-}(700)}$), [**2**/$\mathbf{SiO_{2\text{-}(700)}}$] gives the corresponding monosiloxy complex $[(\equiv SiO)W(\equiv NAr)(=CHtBu)(2,5\text{-}Me_2NC_4H_2)]$ (compound **1**) as the major species (≈90%) along with $[(\equiv SiO)W(\equiv NAr)(CH_2tBu)(2,5\text{-}Me_2NC_4H_2)_2]$ (compound **3**), according to mass balance analysis, IR, and NMR studies as previously observed in the case of the Mo homolog (Scheme 1) (14). Monitoring the grafting step by IR spectroscopy shows that most surface silanols are consumed and that aromatic and alkyl ligands appear as evidenced from the appearance of signals in the 3,100–2,700 ($\nu_{C\text{-}H}$) and 1,600–1,350 ($\delta_{C\text{-}H}$) cm^{-1} regions [supporting information (SI) Fig. S1]. In addition, 0.9 eq of 2,5-dimethylpyrrole is present after grafting, and elemental analyses of the resulting solid ($W = 3.73 \pm 0.05\%_{wt}$, $C = 5.70 \pm 0.1\%_{wt}$, and $N = 0.71 \pm 0.1\%_{wt}$) corresponds to 0.21 mmol/g W, 24 ± 2 carbons, and 2.5 ± 0.5 nitrogen molecules per grafted W, which also is consistent with consumption of most of the surface silanols (0.21 mmol/g W for 0.26 mmol/g SiOH in $SiO_{2\text{-}(700)}$) and formation of **1** as the major surface species, for which 23 C/Mo and 2 N/Mo are expected. Furthermore, the ^1H magic angle spinning (MAS) solid state NMR spectrum, and more convincingly, the constant time (CT) (35, 36) ^1H MAS NMR spectrum (Fig. S2), display the following resonances: 9.0 ($[W] = C\boldsymbol{H}tBu$), 7.0 ($Csp^2\text{-}\boldsymbol{H}$), 6.7 ($Csp^2\text{-}\boldsymbol{H}$), 5.5 (pyrrolyl-$Csp^2\text{-}\boldsymbol{H}$), 3.2 ($C\boldsymbol{H}Me_2$), and 0.9 ($[W] = CHC\boldsymbol{Me}_3$ + pyrrolyl-$Csp^3\text{-}\boldsymbol{H}$ + $CH\boldsymbol{Me}_2$) ppm as expected for **1**, with the signal at 1.9 ppm being associated with the methylene protons in the neopentyl ligand, $[W]\text{-}C\boldsymbol{H}_2tBu$, of **3** (see Scheme 1). Conversely, the ^{13}C cross-polorization (CP) MAS spectrum (Fig. S3 and Table S1) displays the expected signals for **1**, with the exception of the carbenic carbon $[W]{=}\boldsymbol{C}HtBu$, which is not detected, as well as an extra signal at 69 ppm, which can be associated with the methylene carbon $[W]\boldsymbol{C}H_2tBu$ of the neopentyl ligand in **3**. These assignments are

---

Author contributions: F.B., C.C., A.L., L.E., and R.R.S. designed research; F.B., R.B., C.C., A.L., L.E., R.S., T.K., and R.R.S. performed research; F.B., C.C., A.L., L.E., and R.R.S. analyzed data; and F.B., C.C., A.L., L.E., and R.R.S. wrote the paper.

The authors declare no conflict of interest.

This article is a PNAS Direct Submission.

[‡]To whom correspondence should be addressed. E-mail: coperet@cpe.fr.

This article contains supporting information online at www.pnas.org/cgi/content/full/0802147105/DCSupplemental.

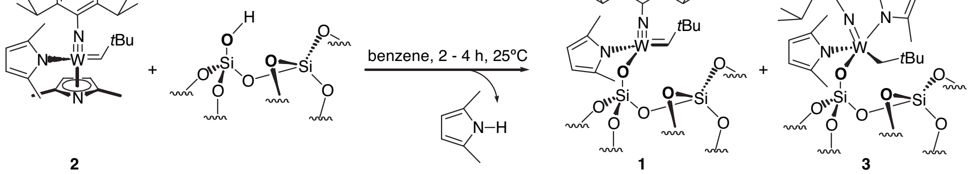

Scheme 1. Formation of [(≡SiO)W(≡NAr)(=CH*t*Bu)(2,5-$Me_2NC_4H_2$)] (compound **1**, 90%) and [(≡SiO)W(=NAr)(CH_2*t*Bu)(2,5-$Me_2NC_4H_2$)$_2$] (compound **3**, 10%) by grafting of [W(≡NAr)(=CH*t*Bu)(2,5-$Me_2NC_4H_2$)$_2$] (compound **2**) with the isolated silanols of $SiO_{2-(700)}$.

confirmed by performing the 2D ^{1}H-^{13}C heteronuclear correlation spectroscopy (HETCOR) solid state NMR on the ^{13}C labeled species [(≡SiO)W(≡NAr)(=*CH*t*Bu)(2,5-$Me_2NC_4H_2$)] (compound **1***), 33% ^{13}C labeled on the α-carbon to W, which clearly shows a correlation associated with the neopentyl carbon [W]-****C**H_2*t*Bu in **3** at 70 ppm and its proton at 1.9 ppm, but which also, and more importantly, displays the neopentylidene carbon signal [W]=***C**H*t*Bu at 260 ppm and its correlation with the corresponding proton [W]=C***H****t*Bu at 9.0 ppm, associated with **1** (Fig. S4). All of these data are consistent with the formation of **1** as the major surface species (90%) via cleavage of the W—N bond by the surface silanol, and the presence of a minor amount of **3**, formed through the competing reaction of addition of a surface silanol with the W=C double bond of **2**.

Contacting [**2/SiO$_{2\text{-}(700)}$**] with propene in a flow reactor (≈82 ml/min^{-1}; ≈420 mol of propene per mol of W per minute) selectively yields ethene and 2-butenes with an initial activity of 0.41 s^{-1} (Fig. S5). Deactivation is slow, and the activity after 1,500 min is still ≈0.1 s^{-1}, so that 25,000 turnovers can be achieved within this time. Although not especially active, **2/SiO$_{2\text{-}(700)}$** displays good stability compared with Mo- and Re-based catalysts, which typically deactivate rapidly (loss of 75% of the activity within 100–400 min). Stability of this catalyst led us to investigate the possibility of observing the NMR spectroscopic signatures of alkene metathesis reaction intermediates, i.e., the propagating carbenes and metallacyclobutane intermediates (10, 37). Therefore, ^{13}C dilabeled ethene was contacted at −196°C with [**2/SiO$_{2\text{-}(700)}$**]. Upon warming the reaction mixture to room temperature, the yellow powder turned red. After 4 h at 25°C, the gas phase contained ≈0.4 eq of 95% ^{13}C monolabeled *t*BuCH=*CH_2. The corresponding solid was then analyzed by solid state NMR. From ^{1}H, ^{13}C CP and ^{1}H-^{13}C HETCOR MAS experiments (Fig. 1), it is clear that intense new peaks have appeared that can be readily assigned as follows (Scheme 2):

Correlation of the ^{1}H and ^{13}C signals at (^{1}H: 9.0/^{13}C: 234 ppm) is fully consistent with a methylidene ligand [W]=***CH***$_2$ in [(≡SiO)W(≡NAr)(=CH_2)(2,5-$Me_2NC_4H_2$)] (compound **4**) (38) resulting from the cross metathesis of the neopentylidene and the ^{13}C di-labeled ethene.

Resonances appearing at (^{1}H: −0.9/^{13}C: −7 ppm) and (^{1}H: 4.0/^{13}C: 100 ppm) correspond to β- and α-carbons of the unsubstituted metallacyclobutane [(≡SiO)W(≡NAr)($CH_2CH_2CH_2$)(2,5-$Me_2NC_4H_2$)] with a trigonal bipyramid geometry (5-TBP). Proton and carbon resonances at 2.0 and 46 ppm, respectively, can

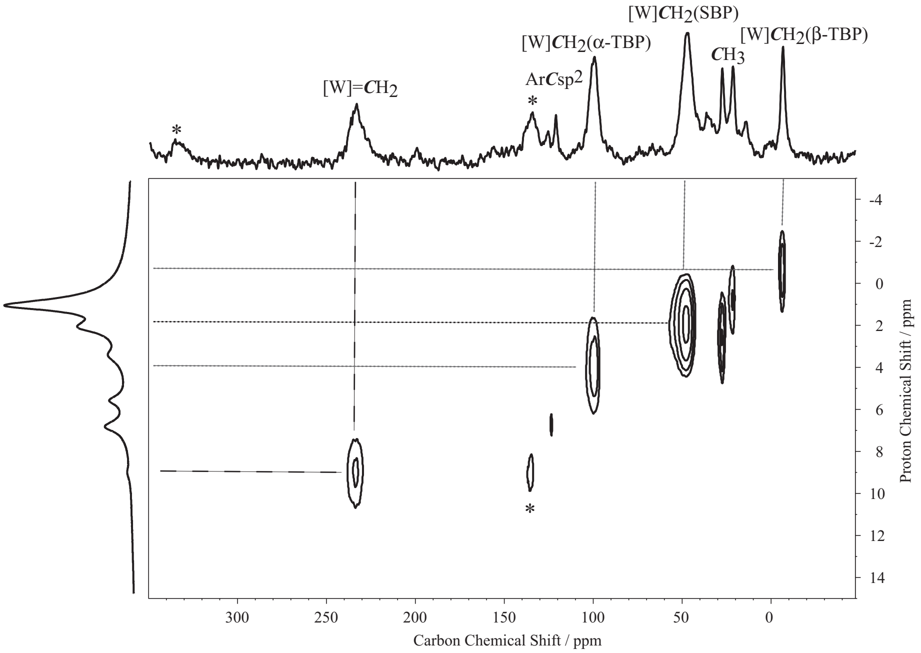

Fig. 1. 2D ^{1}H-^{13}C HETCOR solid state NMR spectrum of [**2/SiO$_{2\text{-}(700)}$**] contacted with ^{13}C dilabeled ethene. This spectrum was acquired under eDUMBO-$1_{12.5}$ (44) homonuclear decoupling (F_1) and SPINAL-64 (45) heteronuclear decoupling (F_2) at ν_1^H = 100 kHz. The contact time for CP and the recycle delay were 500 μs and 2 s, respectively. A total of 48 t_1 points with 512 scans each were collected. A scaling factor (λ_{exp}) of 0.54 was used in F_1 for eDUMBO-$1_{12.5}$ homonuclear decoupling. Asterisks indicate spinning side bands of the alkylidene resonance [W] = *CH_2*. The ^{13}C CP MAS spectrum (512 scans) recorded with a CP step of 500 μs and a recycle delay of 2 s is indicated above the 2D plot. To the left of the 2D plot is shown the ^{1}H single pulse spectrum (eight scans). Dashed and dotted correlations correspond to the methylidene [W]=*CH_2* and metallacyclobutane [W](*$CH_2CH_2CH_2$*) moieties in **4** and **5**, respectively.

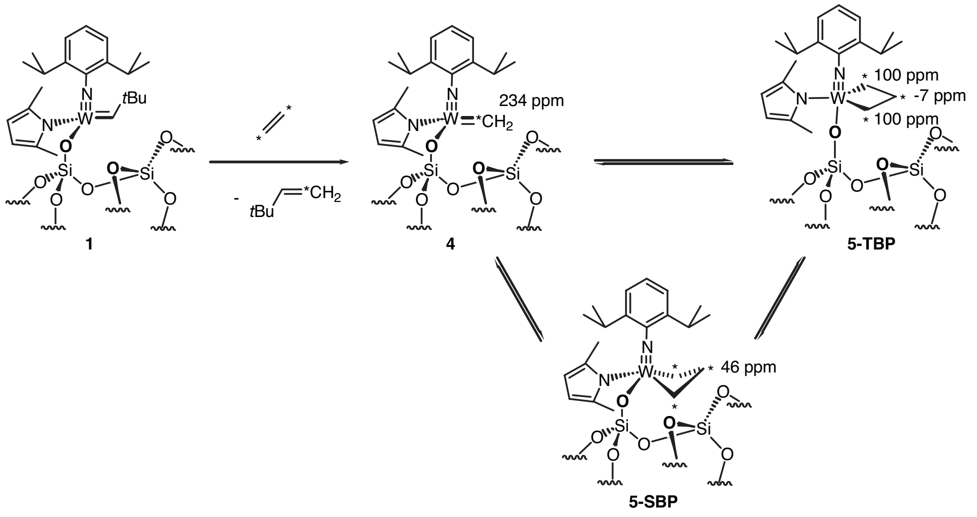

Scheme 2. Formation and NMR spectroscopic signatures of methylidene (compound **4**) and tungstacyclobutane (compound **5**) species by of [(≡SiO)W(≡NAr)(=CH*t*Bu)(2,5-Me$_2$NC$_4$H$_2$)] (1) with ^{13}C dilabeled ethene.

be attributed to the protons and carbons of a metallacyclobutane with a square based pyramid geometry (5-SBP).

Observation of stable metallacyclobutanes in two types of geometries is fully consistent with previous experimental (in solution) (18–25) and theoretical studies (39–43) for d^0 metal complexes. It is also noteworthy that in solution, the SBP/TBP isomer ratio and the reactivity in metathesis are correlated, for a series of isoelectronic metallacyclobutane intermediates of the general formula [(RO)$_2$W(≡NAr)(CH$_2$CH$_2$CH$_2$)], to the electronic properties of the RO ligand as follows: (*i*) for RO = (CF$_3$)$_2$(CH$_3$)CO (the most electron-withdrawing ligand), only the TBP isomer is observed, and the complex is very reactive; (*ii*) for RO = (CF$_3$)(CH$_3$)$_2$CO, a mixture of TBP (a few %) and SBP isomers is observed, and they display intermediate reactivity; and (*iii*) for RO = (CH$_3$)$_3$CO, only the SBP isomer is observed, with very low reactivity because of the high stability of the metallacyclobutane (21, 22). In the case of the active silica supported system reported here, for which the two RO ligands have been replaced by one large siloxy surface ligand and one 2,5-dimethylpyrrolyl ligand, both isomers are observed in roughly equal amounts, and they show good activity (see above). Modulating the ligands in the future by probing the ratio of metallacyclobutane isomers and comparing reactivity opens up a way to access structure-reactivity relationships for heterogeneous alkene metathesis catalysts directly from reaction intermediates.

Moreover, contacting this sample with propene in a flow reactor under the same reaction conditions as those described for [**2**/**SiO$_2$**$_{\text{-(700)}}$] display activities (0.51 s^{-1}) similar to that observed for the original catalyst (0.41 s^{-1} for [**2**/**SiO$_2$**$_{\text{-(700)}}$]) (Fig. S6), albeit with a slightly lower stability. The fact that the methylidene and metallacyclobutane species display similar activity with the well defined silica supported catalyst precursor **1** bearing a neopentylidene ligand clearly suggests that these species are indeed the key reaction intermediates in the alkene metathesis pathway.

Conclusions

We have shown that (*i*) a well defined silica supported W imido alkylidene surface complex [(≡SiO)W(≡NAr)(=CH*t*Bu)(2,5-Me$_2$NC$_4$H$_2$)] (compound **1**), prepared and characterized at a molecular level, displays a good activity, selectivity, and stability in the metathesis of propene; (*ii*) contacting **1** with ^{13}C labeled ethene yields stable methylidene and metallacyclobutane intermediates, resulting from cross metathesis and [2 + 2]-cycloaddition (16, 41, 42); and (*iii*) these species are indeed the key intermediates of the catalytic cycle of alkene metathesis. Overall, these results serve as further evidence that well defined silica-supported systems do behave in a manner similar to homogeneous systems. Direct observation by NMR of these intermediates and their associated spectroscopic signatures is the first step toward a better molecular understanding of heterogeneous olefin metathesis catalysts, and further closes the gap between homogeneous and heterogeneous catalysis. Finally, the design of more efficient catalytic systems may be possible as more information of catalytic intermediates and their stability becomes available (2, 3).

Methods

General Procedures. All experiments were carried out under dry and oxygen-free Ar using either standard Schlenk or glove box techniques for the organometallic synthesis. For the synthesis and treatment of surface species, reactions were carried out using high vacuum lines (1.34 Pa) and glove box techniques. [W(≡NAr)(=CH*t*Bu)(2,5-Me$_2$NC$_4$H$_2$)$_2$] (Ar = 2,6-*i*Pr$_2$C$_6$H$_3$) (compound **2**) was prepared as described previously (34). [(1-^{13}C 33%) W(≡NAr)(=*CH*t*Bu)(2,5-Me$_2$NC$_4$H$_2$)$_2$] (compound **2***) was synthesized as described previously (9) using [(1-^{13}C 33%) *t*Bu^{13}CH$_2$MgCl] as an alkylating agent. [(1-^{13}C 33%) *t*Bu^{13}CH$_2$MgCl] was prepared by mixing (1-^{13}C 99%) *t*Bu^{13}CH$_2$Cl and natural abundance *t*BuCH$_2$Cl followed by the Grignard reaction. Silica (200 m^2/g; Aerosil Degussa) was compacted with distilled water, calcined at 500°C under air for 2 h and treated under vacuum (1.34 Pa) at 500°C for 12 h and then at 700°C for 4 h (support referred to as SiO$_{2\text{-(700)}}$). Benzene and C$_6$D$_6$ (SDS) were distilled from sodium benzophenone ketyl. Propene (99.95%; Scott) and ^{13}C di-labeled ethene (99% ^{13}C; CIL) were purified over R3–11 BASF catalyst/MS 4 Å before use. Cp$_2$Fe (98%; Aldrich) was used as received. Elemental analyses were performed at the Mikroanalythisches Labor Pascher. Infrared spectra were recorded on a Nicolet 550-FT by using an infrared cell equipped with CaF$_2$ windows, allowing *in situ* studies. Typically, 16 scans were accumulated for each spectrum (resolution, 2 cm^{-1}). Products were identified by gas chromatography (GC)/MS. Gas phase analyses were performed on a Hewlett Packard 5890 series II GC apparatus equipped with a flame ionization detector and a KCl/Al$_2$O$_2$ column (50 m × 0.32 mm).

NMR Spectroscopy. ***Liquid state NMR spectroscopy.*** Liquid state NMR spectra were recorded in C$_6$D$_6$ using a Bruker DRX 500 spectrometer and referenced to the residual protonated solvent peaks (δ_H = 7.15 ppm). The amount of 2,5-dimethylpyrrole released during grafting was monitored by quantitative ^{1}H NMR with spin presaturation using Cp$_2$Fe as an internal standard.

Solid state NMR spectroscopy. All solid state NMR spectra were recorded under MAS on a Bruker Avance or Avance II 500 MHz spectrometer with a conventional double-resonance, 4-mm CP MAS probe. The MAS frequency was set to 12.5 kHz for all of the experiments reported here. The proton radiofrequency

(RF) field strength was set to 83 kHz for pulses and 100 kHz during decoupling. For the CP step, the RF field was set to 70 kHz, and for carbon, a ramped RF field was applied on protons and matched to obtain optimal signals. All other experimental details are given in the figure legends. ^1H delayed acquisition spectra including ^1H constant-time spectra were recorded without homonuclear decoupling schemes (36). SPINAL64-^1H (45) heteronuclear decoupling was used in all ^{13}C experiments. An exponential line broadening of 80 Hz was applied before Fourier transform of all ^{13}C experiments. eDUMBO-$1_{12.5}$ (44) homonuclear dipolar decoupling was used for the HETCOR experiment presented in Fig. 1. The experimental scaling factor (λ_{exp}) of 0.54 was obtained by comparing the proton spectra of L-alanine recorded under fast MAS conditions (30 kHz) and under eDUMBO-$1_{12.5}$ decoupling as described previously (44). The samples were filled in a 4-mm zirconia rotor in a glove box and closed with tightly fitting caps. Proton and carbon chemical shifts are reported in ppm downfield from liquid $SiMe_4$ (0 ppm).

Grafting of [W(≡NAr)(=CH*t*Bu)(2,5-$Me_2NC_4H_2$)$_2$] (compound 2) Monitored by *in Situ* IR Spectroscopy. Silica (55 mg) was pressed into a 18-mm self-supporting disk and put into a sealed glass high vacuum reactor equipped with CaF_2 windows. After calcination at 500°C under air for 2 h, the silica disk was treated under vacuum (1.34 Pa) at 500°C for 12 h and then at 700°C for 4 h. The silica support thus obtained ($SiO_{2\text{-}(700)}$, ≈15 μmol SiOH) was then immersed into a benzene (10 ml) solution of [W(≡NAr)(=CHtBu)(2,5-$Me_2NC_4H_2$)$_2$] (**2**) (28 mg, 45 μmol, 3.1 eq) at 25°C for 12 h. After washing the pellet three times with benzene (10 ml) and drying under vacuum (1.34 Pa) at 25°C for 2 h, an IR spectrum of the yellow disk was recorded: 3,066, 3,031, 2,966, 2,936, 2,906, 2,873, 1,613, 1,589, 1,578, 1,473, 1,463, 1,433, 1,387, 1,363 and 1,351 cm^{-1} (Fig. S1). All of the wash solutions were collected and analyzed by ^1H NMR spectroscopy (in C_6D_6), which showed that 2,5-dimethylpyrrole was formed during grafting.

Grafting of [W(≡NAr)(=CH*t*Bu)(2,5-$Me_2NC_4H_2$)$_2$] (2) by Impregnation. A mixture of [W(≡NAr)(=CH*t*Bu)(2,5-$Me_2NC_4H_2$)$_2$] (**2**) (61 mg, 0.10 mmol) and $SiO_{2\text{-}(700)}$ (421 mg, 0.11 mmol SiOH) in benzene (12 ml) was stirred at 25°C for 3 h. After filtration, the volatiles were distilled off, and benzene (≈8 ml) was added. The yellow–orange solid was then washed, filtered and the volatiles distilled off. This was repeated three times, and then the resulting yellow powder was dried under vacuum (1.34 Pa) at 25°C for 2 h to yield [**2/$SiO_{2\text{-}(700)}$**]. All of the filtrate solutions were collected and analyzed by quantitative ^1H NMR spectroscopy (in C_6D_6) using Cp_2Fe (13.3 mg, 71.5 μmol, 1 H) as an internal standard, and 27.4 μmol of 2,5-dimethylpyrrole was formed during grafting (0.9 eq of 2,5-dimethylpyrrole/W_{surf}). Elemental analysis: 3.73$\%_{wt}$ W, 5.70$\%_{wt}$ C, 0.71$\%_{wt}$ N, 24 ± 2 C/Mo, 2.5 ± 0.5 N/Mo.

Grafting of [W(≡NAr)(=*CH*t*Bu)(2,5-$Me_2NC_4H_2$)$_2$] (compound 2*) by Impregnation. This reaction was carried out as described above by using [W(≡NAr)(=*CH*t*Bu)(2,5-$Me_2NC_4H_2$)$_2$] (compound **2***) (33 mg, 0.05 mmol), $SiO_{2\text{-}(700)}$ (232 mg, 0.06 mmol SiOH) and benzene (7 ml), thus yielding a yellow powder, and 44 μmol of 2,5-dimethylpyrrole was formed during grafting (0.9 eq of 2,5-dimethylpyrrole/W_{surf}).

Reaction of ^{13}C Dilabeled Ethene with [2/$SiO_{2\text{-}(700)}$]. To [**2/$SiO_{2\text{-}(700)}$**] (52 mg, 10.6 μmol W) was added ^{13}C dilabeled ethene (65 Torr, 140 μmol, 13 eq), while maintaining the sample at liquid nitrogen temperature. The sample was then brought to room temperature, and its color changed from yellow to red. After 4 h, analysis by gas chromatography indicated the formation of 3.9 μmol of 3,3-dimethylbutene (0.37 eq) with the following isotopomeric composition: 3,3-dimethylbutene (5 ± 5%), 3,3-dimethylbutene-$^{13}C_1$ (95 ± 5%), 3,3-dimethylbutene-$^{13}C_2$ (<1%) and 3,3-dimethylbutene-$^{13}C_3$ (< 1%). The red powder was then dried under vacuum (1.34 Pa) at 25°C for 30 min to yield an orange solid as a mixture of [(≡SiO)W(≡NAr)(=*CH_2)(2,5-$Me_2NC_4H_2$)] (compound **4**) and [(≡SiO)W(≡NAr)(*CH_2*CH_2*CH_2)(2,5-$Me_2NC_4H_2$)$_2$] (compound **5**).

Propene Metathesis in a Flow Reactor. The solid catalyst (40 mg, 8.1 μmol) was loaded in a flow reactor in the glove box, the isolated reaction chamber was then connected to the propene line, the propene pressure was set to 1 bar, and the tubes were flushed with propene for 2 h. The flow rate was set to 82 ml/min (6.6 mol of propene per mol of Mo per second), the temperature was set to 30°C and the opening of the valve corresponds to the beginning of the catalysis. The reaction was monitored by GC using an autosampler.

ACKNOWLEDGMENTS. This work was supported by a Ministère de la Recherche et de l'Education graduate fellowship (to F.B. and R.B.), Centre National de la Recherche Scientifique and École Supérieure Chimie Physique Électronique de Lyon (F.B. and C.C.), French Agence Nationale del la Recherche Young Investigator Fellowship ANR JC05_46372 (to C.C.), and National Science Foundation Grant CHE-0138495 (to R.R.S.). NMR spectra were recorded at the Rhône-Alpes Large Scale Facility for NMR.

1. Mol JC (2004) Industrial applications of olefin metathesis. *J Mol Cat* 213:39–45.
2. Grubbs RH (2006) Olefin-metathesis catalysts for the preparation of molecules and materials. *Angew Chem Int Ed* 45:3760–3765.
3. Schrock RR (2006) Multiple metal-carbon bonds for catalytic metathesis reactions. *Angew Chem Int Ed* 45:3748–3759.
4. Marks TJ (1992) Surface-bound metal hydrocarbyls—Organometallic connections between heterogeneous and homogeneous catalysis. *Acc Chem Res* 25:57–65.
5. Copéret C, Chabanas M, Petroff Saint-Arroman R, Basset J-M (2003) Homogeneous and heterogeneous catalysis: Bridging the gap through surface organometallic chemistry. *Angew Chem Int Ed* 42:156–181.
6. Corma A (2004) Attempts to fill the gap between enzymatic, homogeneous, and heterogeneous catalysis. *Catal Rev Sci Eng* 46:369–417.
7. Thomas JM, Raja R (2006) The advantages and future potential of single-site heterogeneous catalysts. *Top Catal* 40:3–17.
8. Chabanas M, Baudouin A, Copéret C, Basset J-M (2001) A highly active well-defined rhenium heterogeneous catalyst for olefin metathesis prepared via surface organometallic chemistry. *J Am Chem Soc* 123:2062–2063.
9. Chabanas M, *et al.* (2003) Perhydrocarbyl ReVII complexes: Comparison of molecular and surface complexes. *J Am Chem Soc* 125:492–504.
10. Copéret C (2004) Molecular design of heterogeneous catalysts: The case of olefin metathesis. *New J Chem* 28:1–10.
11. Blanc F, *et al.* (2006) Surface versus molecular siloxy ligands in well-defined olefin metathesis catalysts: [{$(RO)_3SiO$}Mo(=NAr)(=CH*t*Bu)(CH_2*t*Bu)]. *Angew Chem Int Ed* 45:1216–1220.
12. Rhers B, *et al.* (2006) A well-defined, silica-supported tungsten imido alkylidene olefin metathesis catalyst. *Organometallics* 25:3554–3557.
13. Blanc F, *et al.* (2007) Highly active, stable, and selective well-defined silica supported Mo imido olefin metathesis catalysts. *J Am Chem Soc* 129:1044–1045.
14. Blanc F, *et al.* (2007) Dramatic improvements of well-defined silica supported Mo-based olefin metathesis catalysts by tuning the N-containing ligands. *J Am Chem Soc* 129:8434–8435.
15. Copéret C (2007) Design and understanding of heterogeneous alkene metathesis catalysts. *Dalton Trans* 47:5498–5504.
16. Herisson JL, Chauvin Y (1971) Transformation catalysis of olefins by tungsten complexes 2. Telomerization of cyclic olefins in presence of acyclic olefins. *Makromol Chem* 141:161–176.
17. Kress J, Osborn JA (1992) Proof of the carbene-olefin intermediate in tungsten-containing metathesis catalysts with the metal in a higher oxidation state. *Angew Chem Int Ed* 31:1585–1587.
18. Schrock RR, *et al.* (1988) Preparation and reactivity of several alkylidene complexes of the type W(CHR')(N-2,6-C_6H_3-*iso*-Pr_2)$(OR)_2$ and related tungstacyclobutane complexes. Controlling metathesis activity through the choice of alkoxide ligand. *J Am Chem Soc* 110:1423–1435.
19. Feldman J, Murdzek JS, Davis WM, Schrock RR (1989) Reaction of neopentylidene complexes of the type M(CH-*t*-Bu)(N-2,6-C_6H_3-*i*-Pr_2)$(OR)_2$ (M = W, Mo) with methyl acrylate and N,N-dimethylacrylamide to give metallacyclobutane complexes. *Organometallics* 8:2260–2265.
20. Feldman J, Davis WM, Schrock RR (1989) Trigonal-bipyramidal and square-pyramidal tungstacyclobutane intermediates are both present in systems in which olefins are metathesized by complexes of the type W(CHR')(N-2,6-C_6H_3-*iso*-Pr_2)$(OR)_2$. *Organometallics* 8:2266–2268.
21. Feldman J, Davis WM, Thomas JK, Schrock RR (1990) Preparation and reactivity of tungsten(VI) metallacyclobutane complexes. Square pyramids versus trigonal bipyramids. *Organometallics* 9:2535–2548.
22. Feldman J, Schrock RR (1991) Recent advances in the chemistry of d^0 alkylidene and metallacycobutane complexes. *Prog Inorg Chem* 39:1–74.
23. Tsang WCP, Schrock RR, Hoveyda AH (2001) Evaluation of enantiomerically pure binaphthol-based molybdenum catalysts for asymmetric olefin metathesis reactions that contain 3,3'-diphenyl- or 3,3'-dimesityl-substituted binaphtholate ligands. Generation and decomposition of unsubstituted molybdacyclobutane complexes. *Organometallics* 20:5658–5669.
24. Tsang WCP, *et al.* (2003) Alkylidene and metalacyclic complexes of tungsten that contain a chiral biphenoxide ligand. Synthesis, asymmetric ring-closing metathesis, and mechanistic investigations. *J Am Chem Soc* 125:2652–2666.
25. Tsang WCP, *et al.* (2004) Investigations of reactions between chiral molybdenum imido alkylidene complexes and ethylene: Observation of unsolvated base-free methylene complexes, metalacyclobutane and metalacyclopentane complexes, and molybdenum(IV) olefin complexes. *Organometallics* 23:1997–2007.
26. Romero PE, Piers WE (2005) Direct observation of a 14-electron ruthenacyclobutane relevant to olefin metathesis. *J Am Chem Soc* 127:5032–5033.
27. Anderson DR, Hickstein DD, O'Leary DJ, Grubbs RH (2006) Model compounds of ruthenium-alkene intermediates in olefin metathesis reactions. *J Am Chem Soc* 128:8386–8387.

28. Wenzel AG, Grubbs RH (2006) Ruthenium metallacycles derived from 14-electron complexes. New insights into olefin metathesis intermediates. *J Am Chem Soc* 128:16048–16049.
29. Romero PE, Piers WE (2007) Mechanistic studies on 14-electron ruthenacyclobutanes: Degenerate exchange with free ethylene. *J Am Chem Soc* 129:1698–1704.
30. Siaj M, *et al.* (2004) Dissociation of acetaldehyde on β-Mo_2C to yield ethylidene and oxo surface groups: A possible pathway for active site formation in heterogeneous olefin metathesis. *J Am Chem Soc* 126:9514–9515.
31. Salameh A, *et al.* (2007) CH_3ReO_3 on γ-Al_2O_3: Understanding its structure, initiation, and reactivity in olefin metathesis. *Angew Chem Int Ed* 46:3870–3873.
32. Salameh A, *et al.* (2008) CH_3ReO_3 on γ-Al_2O_3: Activity, selectivity, active site and deactivation in olefin metathesis. *J Catal* 253:180–190.
33. Chabanas M (2001) PhD thesis (Université Lyon, Lyon, France), pp 1–167.
34. Kreickmann T, Arndt S, Schrock RR, Mueller P (2007) Imido alkylidene bispyrrolyl complexes of tungsten. *Organometallics* 26:5702–5711.
35. Lesage A, Duma L, Sakellariou D, Emsley L (2001) Improved resolution in proton NMR spectroscopy of powdered solids. *J Am Chem Soc* 123:5747–5752.
36. Blanc F, *et al.* (2006) Better characterization of surface organometallic catalysts through resolution enhancement in proton solid state NMR spectra. *Inorg Chem* 45:9587–9592.
37. Blanc F, Copéret C, Lesage A, Emsley L (2008) High resolution solid state NMR spectroscopy in surface organometallic chemistry: Access to molecular understanding of active sites of well-defined heterogeneous catalysts. *Chem Soc Rev* 37:518–526.
38. Arndt S, Schrock RR, Mueller P (2007) Synthesis and reactions of tungsten alkylidene complexes that contain the 2,6-dichlorophenylimido ligand. *Organometallics* 26:1279–1290.
39. Goumans TPM, Ehlers AW, Lammertsma K (2005) The asymmetric Schrock olefin metathesis catalyst. A computational study. *Organometallics* 24:3200–3206.
40. Poater A, *et al.* (2006) DFT calculations of d(0) M(NR)(CH*t*Bu)(X)(Y) (M = Mo, W; R = CPh_3, 2,6-*i*Pr-C_6H_3; X and Y = CH_2*t*Bu, O*t*Bu, OSi(O*t*Bu)$_3$) olefin metathesis catalysts: Structural, spectroscopic and electronic properties. *Dalton Trans* 25:3077–3087.
41. Solans-Monfort X, Clot E, Copéret C, Eisenstein O (2005) d(0) Re-based olefin metathesis catalysts, Re(=CR)(=CHR)(X)(Y): The key role of X and Y ligands for efficient active sites. *J Am Chem Soc* 127:14015–14025.
42. Poater A, *et al.* (2007) Understanding d(0)-olefin metathesis catalysts: Which metal, which ligands. *J Am Chem Soc* 129:8207–8216.
43. Handzlik J (2007) Theoretical investigations of isolated Mo(VI) and Mo(IV) centers of a molybdena-silica catalyst for olefin metathesis. *J Phys Chem C* 111:9337–9348.
44. Elena B, de Paepe G, Emsley L (2004) Direct spectral optimisation of proton-proton homonuclear dipolar decoupling in solid-state NMR. *Chem Phys Lett* 398:532–538.
45. Fung BM, Khitrin AK, Ermolaev K (2000) An improved broadband decoupling sequence for liquid crystals and solids. *J Magn Reson* 142:97–101.

CHEMISTRY